JACS
JOURNAL OF THE AMERICAN CHEMICAL SOCIETY

ARTICLE

pubs.acs.org/JACS

Impact of Distinct Chemical Structures for the Development of a Methamphetamine Vaccine

Amira Y. Moreno, Alexander V. Mayorov, and Kim D. Janda*

Departments of Chemistry and Immunology, the Skaggs Institute for Chemical Biology, and the Worm Institute of Research and Medicine (WIRM), The Scripps Research Institute, 10550 N. Torrey Pines Road, La Jolla, California 92037, United States

Supporting Information

ABSTRACT: (+)-Methamphetamine (METH) use and addiction has grown at alarming rates over the past two decades, while no approved pharmacotherapy exists for its treatment. Immunopharmacotherapy has the potential to offer relief through producing highly specific antibodies that prevent drug penetration across the blood−brain barrier thus decreasing reinforcement of the behavior. Current immunotherapy efforts against methamphetamine have focused on a single hapten structure, namely linker attachment at the aromatic ring of the METH molecule. Hapten design is largely responsible for immune recognition, as it affects presentation of the target antigen and thus the quality of the response. In the current paper we report the systematic generation of a series of haptens designed to target the most stable conformations of methamphetamine as determined by molecular modeling. On the basis of our previous studies with nicotine, we show that introduction of strategic molecular constraint is able to maximize immune recognition of the target structure as evidenced by higher antibody affinity. Vaccination of GIX$^+$ mice with six unique METH immunoconjugates resulted in high antibody titers for three particularly promising formulations (45−108 μg/mL, after the second immunization) and high affinity (82, 130, and 169 nM for MH2, MH6, and MH7 hapten-based vaccines, respectively). These findings represent a unique approach to the design of new vaccines against methamphetamine abuse.

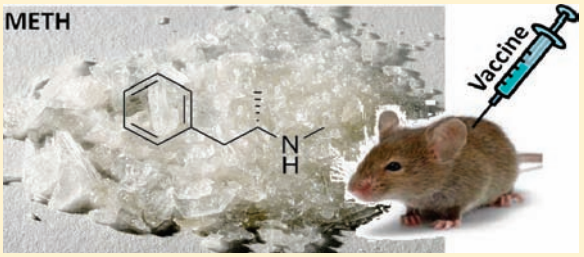

INTRODUCTION

(+)-Methamphetamine (METH) use and addiction in the United States has grown at alarming rates over the past two decades,[1] burdening the US economy with an estimated medical, lost productivity, and law enforcement cost of $23.4 billion.[2] The effect of methamphetamine on the dopaminergic signaling pathway is largely responsible for its powerful rewarding[3] as well as addictive properties. Furthermore, the high rate of relapse in the patients undergoing methamphetamine withdrawal underscores the level of challenge in development of an effective therapy for methamphetamine addiction.[4] Currently, psychosocial and behavioral management is the only available treatment.

Development of an efficacious pharmacotherapy is of pressing concern, yet the complexity of drug action on the brain circuitry has presented a significant challenge.[5] Immunopharmacotherapy uses an alternative approach wherein antibodies are used to prevent drug distribution to brain receptors, thus decreasing reinforcement of the behavior. Previous immunotherapy efforts have targeted various drugs of abuse[6] and importantly, antinicotine[7] and anticocaine vaccines[8] have shown titer dependent efficacy during clinical trials. Active vaccination efforts against METH have largely proven ineffective during behavioral testing,[9] providing an impetus for development of more effective approaches to a vaccine against methamphetamine addiction.

The success of any small molecule active vaccine is intimately determined by three factors: antibody specificity, affinity, and antibody concentration (titer). Small molecules, such as METH, require appendage to carrier macromolecules in order to elicit an immune response. The chemical positioning of a linker to the target antigen has proven to be crucial for proper immune stimulation both in terms of amount of antibody elicited and antibody specificity.[10] Thus, proper hapten design is critical for immune recognition, as it affects presentation of the target antigen and thus quality of the response.[10,11] Immunotherapy efforts against methamphetamine have largely focused on the use of a single scaffold, i.e., linker attachment at the aromatic ring of the parent molecule (Figure 1).[12] Variations of linker identity and length have allowed for some immune regulation, yet vaccination of this structure has proven largely ineffective during behavioral testing.[9] The sole exception is a METH vaccine based on a self-adjuvanting peptide construct wherein efficacy was independent of hapten design and was determined by the presence of an additional T cell epitope from tetanus toxin.[13]

Based on the poor response obtained from active vaccination, the bulk of the literature to date has focused on the use of anti-METH monoclonal antibodies, i.e., passive vaccination, which when administered has shown reduction of METH-associated behavior.[14] Despite this potential efficacy, the expense of passive vaccination is of concern. Active vaccination generates

Received: September 30, 2010
Published: April 07, 2011

dx.doi.org/10.1021/ja108807j | J. Am. Chem. Soc. 2011, 133, 6587–6595

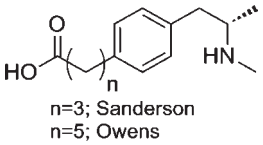

Figure 1. Previously reported haptens for active anti-METH vaccines.

immunological memory to repeated exposure of the drug conjugate. Thus, the cost effectiveness of treatment is increased, allowing for longer sustained protection with minimal compliance and could be a viable approach for relapse prevention.

As a path forward for the development of a METH vaccine, we report the systematic generation of a series of unique chemical structures designed to target the most stable conformations of methamphetamine in solution as determined by molecular modeling. We present the serological analysis of GIX^+ mice following vaccination with six unique METH haptens, with three of them being particularly promising, and elaborate on the impact of these findings on the design of future vaccines against methamphetamine abuse.

RESULTS AND DISCUSSION

Theoretical Calculations. Vital to constrained hapten design, the conformational profile of the protonated form of (+)-methamphetamine was examined using MacroModel 9.1 equipped with Maestro 7.5 graphical interface (Schrödinger, Portland, OR). Structures were minimized using the OPLS_2005 force field[15] and the Polak−Ribiere conjugate gradient. Aqueous solution conditions were simulated using the continuum dielectric water solvent model (GB/SA).[16] The key dihedral angles in these simulations were denoted as Φ (C^1−N−C^2−C^3) and Ψ (N−C^2−C^3−Ph). As expected, two dihedral drive simulations on the global minimum of the methamphetamine structure showed the lowest energy conformation that positioned the largest substituents anti to one another (Φ ≈ 180°, Ψ ≈ 180°) with two separate gauche-anti conformers (Φ ≈ 180°, Ψ ≈ ± 60° and Φ ≈ ± 60°, Ψ ≈ 180°) also identified as potential energy sinks (Figure 2). These findings allowed us to identify two approaches to constructing conformationally constrained methamphetamine haptens: (1) C^1−C^4 constraint and (2) C^1-phenyl ring constraint (Figure 3). The former approach was convenient to achieve by using a commercially available, appropriately ornamented piperazine template, while the tetrahydroisoquinoline (THIQ) template was found to be suitable for establishing the latter type of dihedral constraint, both by matching the dihedral angles of the energetically favored (−) gauche-anti conformer (Φ ≈ −60°, Ψ ≈ 180°) and by possessing a sufficient basicity of the requisite secondary amine nitrogen. Thus, the designed haptens fall into one of three categories as determined by the identity of their core structures. MH1 and MH2 present an inherently anti-anti constrained piperazine nucleus, MH3 and MH5 are derivatized tetrahydroisoquinolines, and finally MH6 and MH7 are functionalized versions of the unconstrained methamphetamine molecule (Figure 4).

The global minima of (+)-methamphetamine and the hapten core structures MH1−3, MH5−7 (in their respective protonated forms) were obtained using the hybrid Monte Carlo/low frequency mode simulations (MCMM/LMCS) procedure as implemented in Macromodel[17] using the energy minimization routine as described above. To simplify the computational experiments and the subsequent comparison of structures, the alkylsulfhydryl linker HS-$(CH_2)_4$ was removed in the simulations of all hapten structures, except for MH6, where only the terminal sulfhydryl group was removed. Superpositions of the minimized parent molecule with all haptens were performed by alignment of four key loci: the amine nitrogen, the *N*-Me, the C^2-carbon atom, and the C^3-carbon atom. Superpositions of the constrained haptens MH1(R) and MH2(R), as well as unconstrained haptens MH6(S) and MH7(S), with the global minimum conformation of methamphetamine showed an

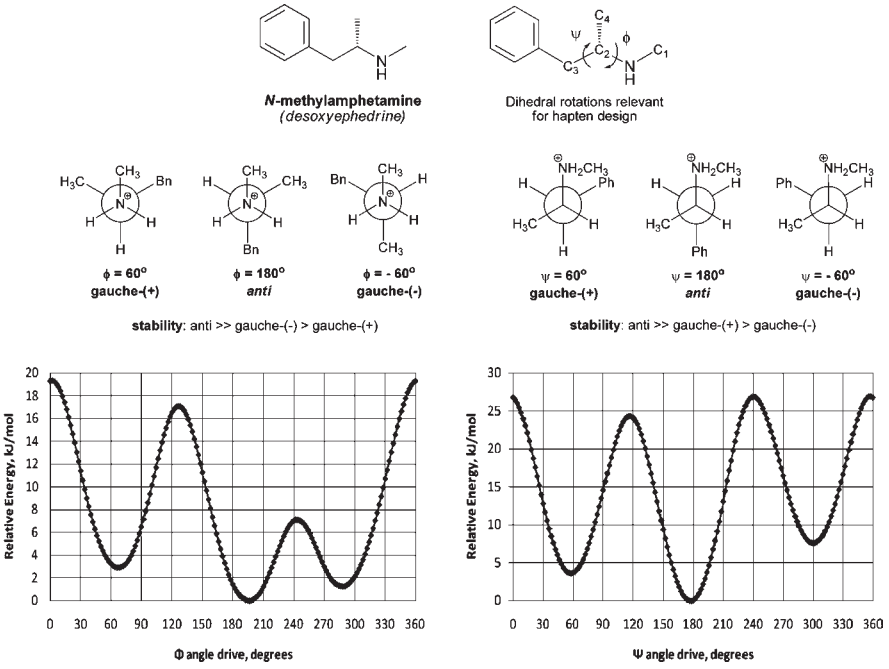

Figure 2. The conformational profile of *N*-methylamphetamine (Φ/ψ), as determined by dihedral drive/OPLS_2005-GB/SA simulations. Potential energy is expressed in relative terms to the following minima: −148.208 kJ/mol (Φ = 196°) and −148.197 kJ/mol (Ψ = 178°).

dx.doi.org/10.1021/ja108807j |*J. Am. Chem. Soc.* 2011, 133, 6587–6595

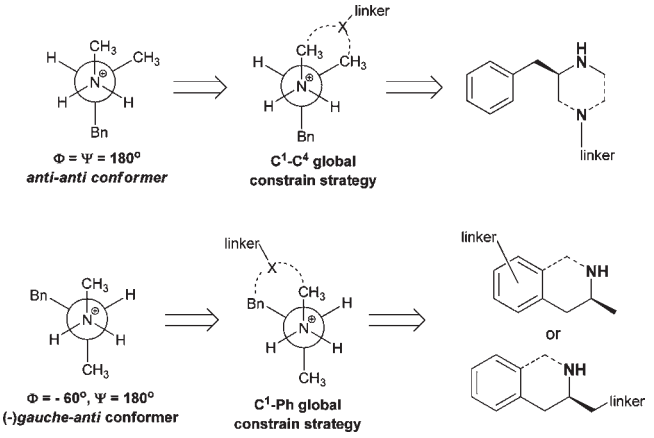

Figure 3. Two strategies toward conformationally constrained methamphetamine haptens.

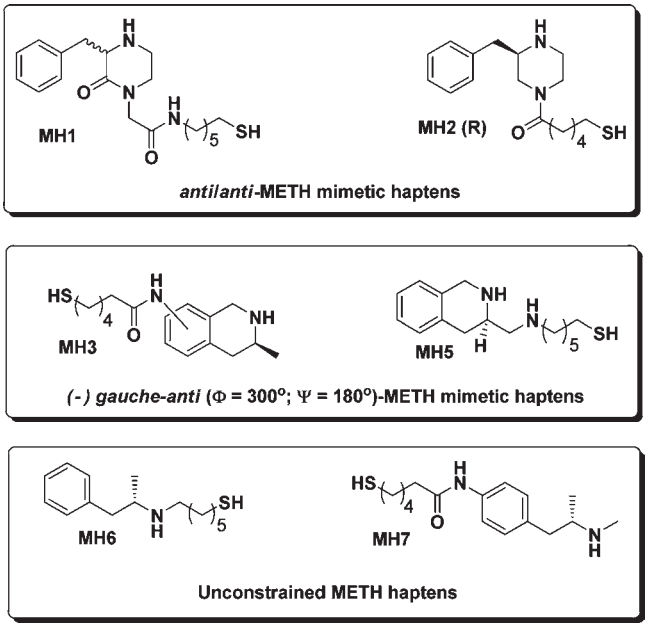

Figure 4. Designed hapten structures targeting (+)-methamphetamine.

excellent fit (Figures 5 and 6). Similarly, MH3(S) and MH5(R) structures were determined to share a matching core conformation with the (−) gauche-anti conformer of methamphetamine (Figure 7). Thus, each of the two constrained core categories mimics a distinct low energy conformation of the target structure. Deviations in conformation for all superpositions were calculated as a root-mean-square (rms) and were found to be reasonably low at <0.15, indicating a good fit.

It is important to point out that we considered the presence of basic secondary amine functionality in our haptens to be vital for the success of the methamphetamine vaccine. While the basicity of the acyl-piperazine core-based haptens MH1 and MH2 (pK_a = 11.12 for piperidine, 9.82 for piperazine)[18] was expected to be similar to that of methamphetamine (pK_a = 10.1),[19] the ionization constant of the THIQ template has been shown be somewhat lower ($pK_a \approx 9.30$).[20] We hypothesized that both core structures were basic enough to ensure sufficient protonated state population at the physiological pH (7.4), giving rise to antibodies targeting the methamphetamine

Figure 5. Stereoview of superposition of the global minima of (+)-methamphetamine (red), MH1 (blue) and MH2 (gold). rmsd (MH1−METH) = 0.15, rmsd (MH2−METH) = 0.11. Hydrogens are omitted for clarity.

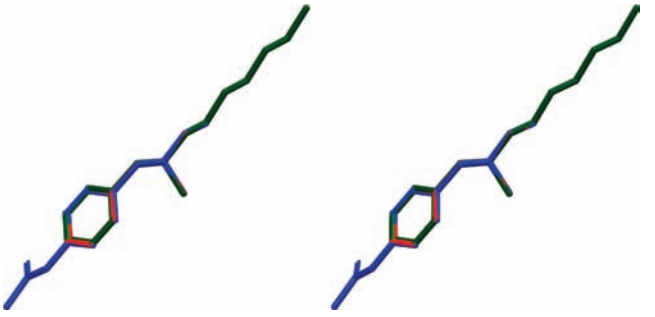

Figure 6. Stereoview of superposition of the global minima of (+)-methamphetamine (red), MH6 (green), and MH7 (blue). rmsd (MH6−METH) = 0.01, rmsd (MH7−METH) = 0.001. Hydrogens are omitted for clarity.

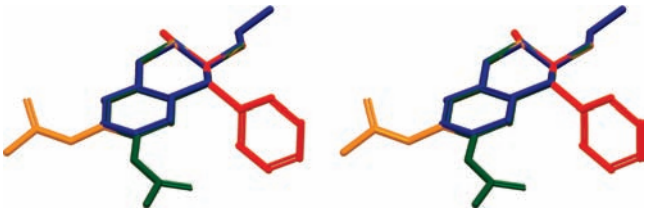

Figure 7. Stereoview of superposition of the (−) gauche/anti conformation of (+)-methamphetamine (red), and the global minima of two regioisomers of MH3 (green and gold) and MH5 (blue). rmsd (MH3−METH) = 0.06, rmsd (MH5−METH) = 0.02. Hydrogens are omitted for clarity.

structure in its protonated form. A possible complication from using a basic amine linker in the MH5 hapten was recognized, due to the uncertainty of its protonation behavior. Using the NMR work of Beaumont and co-workers on the structurally related aminomethyl-THIQ analogues[20] as a guide, we concluded that the linker nitrogen should be expected to be somewhat more basic than the THIQ core nitrogen (pK_a (dimethylamine) = 10.73 vs pK_a (THIQ) = 9.3).[18] Computational pK_a prediction as implemented in Schrodinger Epik program[21] supported this hypothesis, yielding the pK_a estimates at 9.62 for the linker amino group, and 6.72 for the THIQ core. Regardless, comparison of the global minima of both protonated forms showed near identical conformations (rmsd =0.055) (not shown). In addition, as pointed out by Beaumont and co-workers,[20] intramolecular hydrogen bonding between the protonated and the free amino groups is likely and was in fact found by the computer

dx.doi.org/10.1021/ja108807j |J. Am. Chem. Soc. 2011, 133, 6587–6595

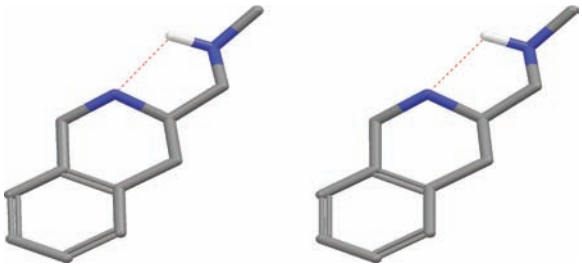

Figure 8. Stereoview of the global minimum of the protonated form of MH5, showing the putative intramolecular hydrogen bonding. Hydrogens are omitted for clarity.

simulations in both protonated forms (Figure 8), which suggested a certain degree of proton sharing between the amino groups, which we deemed both acceptable and interesting to pursue as a structural feature of a methamphetamine hapten.

Hapten Design. Our strategy for hapten design consisted of three main veins: (1) to focus the response on the lowest energy conformations of methamphetamine as elucidated by molecular modeling, (2) to mimic the most psychoactive enantiomer of the parent molecule, and (3) to maximize hapten loading efficacy via a noncompeting bioconjugation technique.

First, we hypothesized that targeting of the lowest energy conformations could be achieved by either a constrained or unconstrained approach. Unconstrained structures would effectively mimic the target by theoretically converging onto the same energy conformation of the parent structure. However, depending on the energy expenditure required to go from one potential energy sink to another, a series of structures could exist through time. Previous reports on development of small molecule haptens for vaccines against nicotine abuse have provided compelling evidence that application of conformational constraints can be used to reduce the hapten's internal rotational degree of freedom, thus minimizing the entropic loss upon antibody binding.[6a,22] Methamphetamine, like nicotine, is a small molecule with ample degrees of freedom provided by rotation along its sigma bonds. Thus, we hypothesized that rational introduction of a strategic molecular constraint would be able to "guide" the immune response toward the most stable and, thus, most prevalent conformation of the parent structure. On the basis of our modeling experiments, vide supra, we proposed two specific ways to introduce molecular constraint in order to target two distinct low energy conformations for methamphetamine. This allowed us to categorize our haptens based on the identity of their core structures. MH1 and MH2 present a constrained piperazine nucleus, MH3 and MH5 are constrained based on a tetrahydroisoquinoline scaffold, and finally MH6 and MH7 are linker-functionalized versions of the free rotating methamphetamine molecule.

Second, it is well established in the literature that (+)-methamphetamine is about a five times more potent stimulant drug than its (−)-methamphetamine enantiomer, thus increasing its liability for abuse.[23,24] During our hapten design, we hypothesized that paying special attention to the stereochemical requirements of the more potent enantiomer of methamphetamine would allow for superior immune tuning. Thus, the design of our haptens focused on targeting the appropriate (+)-configuration.

Finally, we hypothesized that maximizing hapten load onto the carrier proteins could provide more potent immune stimulation. Previous work focused on the use of carbodiimide activation of carboxylic acid haptens for attachment to free amino groups in the lysine residues of carrier proteins.[9] Yet, we argue that this type of chemistry may not be optimal when dealing with a structure, such as methamphetamine, which itself presents a reactive secondary amine. This could lead to loss of material to oligomerization-type reactions as well as unreliable conjugation. We have opted instead for an orthogonal conjugation technique using a maleimide spacer with pH-modulated thiol selectivity. The robustness of this conjugation method is highlighted by similar conjugation efficiencies for all haptens tested, determined by the number of hapten copies on the carrier, which we suspected to have an impact on the efficacy of immune stimulation toward a particular target. Efficacy of conjugation was monitored using MALDI-TOF MS for hapten coupling to bovine serum albumin (BSA) under the same conditions, and all haptens were found to produce similar coupling rates at 24−29 copies per BSA molecule.

Synthetic Preparation of Haptens. All haptens were prepared from commercially available starting materials using standard reaction conditions. Full synthetic details and characterization of all haptens are given in the Supporting Information. We note that whenever possible we obtained enantiomerically pure materials to match the most active stereoisomer of methamphetamine. However, MH1, MH3, and MH5 were synthesized in racemic form and were not further resolved. Additionally, MH3 yielded two regioisomers that were not separated further, as they only vary at the site of linker attachment within the aromatic ring (positions 6 and 7, Supporting Information). Molecular modeling of both regioisomers deemed this not to be critical for immune presentation. A brief description of each synthesis is shown, vide infra.

MH1 and MH2(R), constrained anti-anti METH mimetics, were synthesized by functionalization of the commercially available piperazine cores with the appropriate linker, 6-(tritylthio)hexan-1-amine for MH1 and 6-(tritylthio)hexanoic acid for MH2. Carbodiimide activation chemistry was used for linker coupling; this was followed by acid deprotection of the trityl group to yield the desired haptens (Scheme 1). In short, we took advantage of the fact that the piperazine core needed to prepare MH2 was commercially available as either enantiomer, thus allowing easy access to structures that targeted both the (+) and (−) enantiomers of methamphetamine. This was significant, as it would allow us to gauge the importance of retaining the stereochemical requirements of our target, (+)-methamphtamine, the most active isomer, during hapten design. In contrast for the MH1 hapten, starting material was only available for the opposite enantiomer; thus, to access both isomers, racemization was accomplished using 1,8-diazabicycloundec-7-ene (DBU) and heat (see Supporting Information). The two isomers of MH1 were not further resolved, as we have previously shown how the immune system can readily generate antibodies able to selectively recognize either antipode from a racemic synthetic hapten.[25]

The syntheses of tetrahydroisoquinoline (THIQ) haptens MH3 and MH5 are shown within Scheme 2. The synthesis of MH3 was initiated with indium-mediated reduction of 3-methylisoquinoline to the corresponding 1,2,3,4-tetrahydroisoquionline, **1**; this was followed by aromatic nitration, which resulted in **2** as a mixture of regioisomers at positions 6 and 7, as stated, vide supra, that were not further resolved. Boc-protection of the reactive secondary amine of **2** followed by reduction of the nitro moiety granted **3** and allowed for facile coupling of the 6-(tritylthio)-hexanoic acid linker. Global acidic deprotection provided MH3. The synthesis of MH5 was initiated with the reduction and reoxidation of the carboxylic acid from commercially available (*R*)-N-Boc-1,2,3,4-tetrahydroisoquinoline-3-carboxylic acid

Scheme 1. Synthesis of Constrained Anti-Anti METH Mimetic Haptens, MH1/MH2

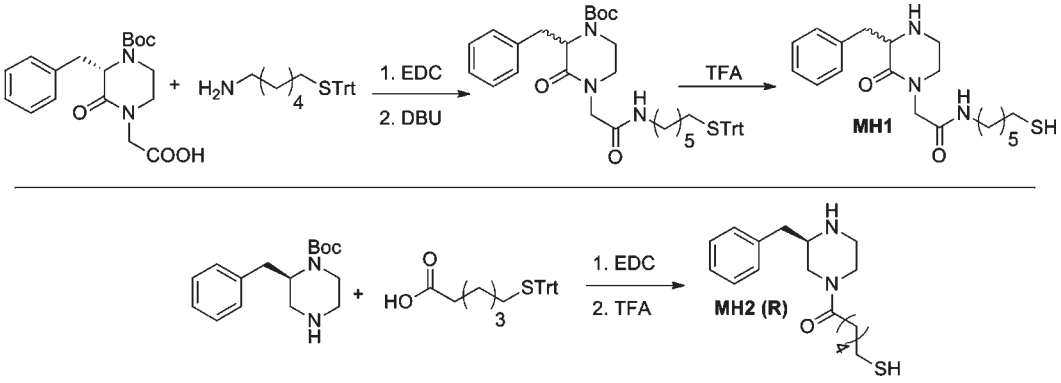

Scheme 2. Synthetic Routes toward (−) Gauche-Anti METH Mimetic Haptens, MH3/MH5

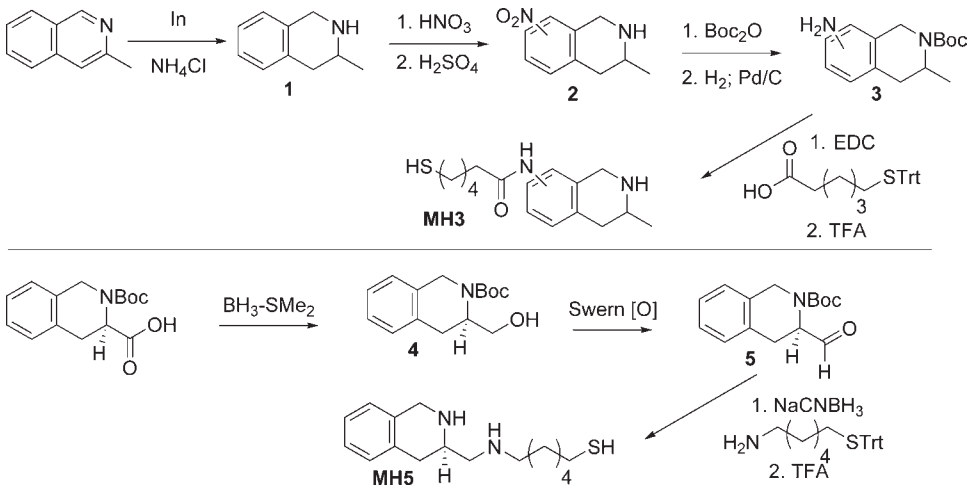

(Fluka), providing **5**. Aldehyde **5** was subjected to reductive amination using sodium cyanoborohydride and 6-(tritylthio)-hexan-1-amine; this was followed by global acidic deprotection to yield MH5.

The synthesis of the unconstrained hapten cores proceeded in the following manner. MH6 was accessed by simple N-alkylation of (+)-amphetamine with 6-(tritylthio)hexyl methanesulfonate followed by acid deprotection. The synthesis of MH7 was more involved and began from (+)-methamphetamine that was found to be quite volatile as its free base, thus requiring protection of the secondary amine with trifluoroacetic anhydride in order to allow for easier handling. Thus, aromatic nitration gave rise to para-substituted trifluoroacetamide methamphetamine, **6**, as the major product, which was separated using silica chromatography. Reduction of the nitro functionality yielded **7**, which was followed by linker coupling using 6-(tritylthio)hexanoic acid, providing **8**. Base/acid deprotection of the trifluoroacetamide and trityl moieties gave the final product MH7.

Characterization of anti-METH Antibodies. As stated, success of active vaccination is contingent upon both the magnitude of the response as well as the affinity and specificity of the antibodies (Abs) generated. The magnitude of the immune response was initially assessed by ELISA on microtiter plates coated with either MH6− or MH7−BSA conjugates. It was immediately apparent that the site of linker attachment played an important role in determining relative cross-reactivity, i.e., MH3 preferentially identified MH7, while MH5 preferentially identified MH6. This bias was removed by use of equilibrium dialysis, a solution-based assay we feel more closely resembles the in vivo interaction. All binding constants as well as antibody concentrations reported were calculated from a solution-based radioimmunoassay (RIA) and normalized, thus allowing for direct comparison of values between test groups.

We hypothesized that mimicking of the target structure via either introduction of strategic molecular constraint or effective functionalization would maximize immune recognition of the target structure as demonstrated by higher antibody affinity and specificity. Gratifyingly, the highest affinity anti-METH Abs were observed with constrained hapten MH2(R), an anti-anti METH mimetic as determined by molecular modeling, followed by unconstrained haptens MH6 and MH7. By the end of the study, polyclonal responses had an affinity well within the range of previous anti-methamphetamine mAbs tested (10−250 nM).[26] Nonetheless, unconstrained haptens MH6 and MH7 produced antibody concentrations in the 150−220 μg/mL range which corresponds to 3× and 2× larger responses than that of constrained hapten MH2(R). To put these values into perspective, a nicotine vaccine that has advanced to clinical trials generated antibodies in rats within the same range (184 μg/mL).[27] Furthermore, these values are about 2 orders of magnitude higher than those reported by Duryee et al.[13] wherein vaccination showed moderate effects in the rates of

dx.doi.org/10.1021/ja108807j |J. Am. Chem. Soc. 2011, 133, 6587–6595

Scheme 3. Synthetic Routes toward Unconstrained METH Haptens, MH6/7

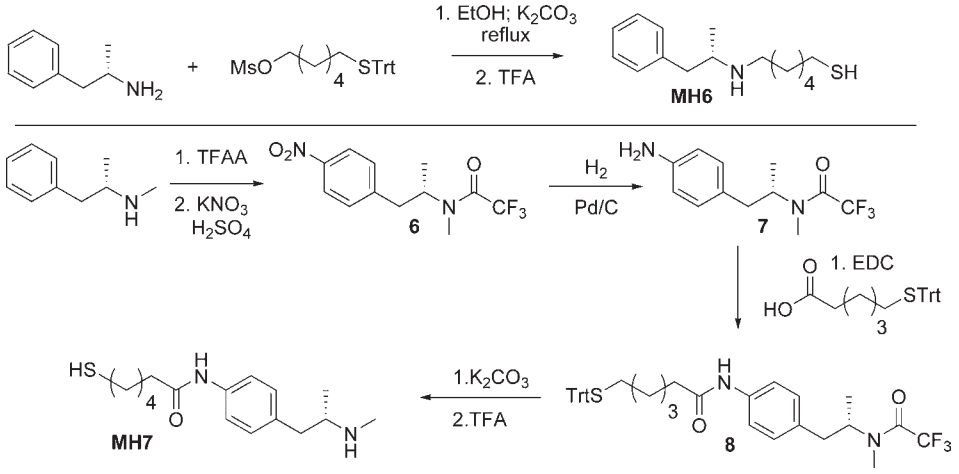

Table 1. Average Relative Affinities of Antisera from Immunized Mice against Amphetamine and Methamphetamine As Determined by Equilibrium Dialysis

immunized antigen		[abs] ± SE μg/mL	(+)-METH K_D(μM)	(+)-amph K_D(μM)
MH2(R)	first bleed	70.83 ± 4.05	0.218 ± 0.055	1.267 ± 0.309
	second bleed	44.53 ± 2.54	0.082 ± 0.018	0.356 ± 0.093
MH6	first bleed	220.13 ± 19.69	0.266 ± 0.034	1.12 ± 0.171
	second bleed	107.83 ± 7.22	0.130 ± 0.019	0.724 ± 0.082
MH7	first bleed	152.53 ± 9.08	0.152 ± 0.011	23.73 ± 3.52
	second bleed	89.85 ± 11.89	0.169 ± 0.023	22.54 ± 4.70

methamphetamine intravenous self-administration. On the other hand, vaccination with MH1 as well as the tetrahydroisoquinoline (THIQ) haptens MH3 and MH5 produced antibodies with minimal affinity for METH in solution (>50 μM) and thus were discarded from future testing.

These findings suggest that targeting the (−) gauche/anti conformation of methamphetamine does not appear to be as effective at raising an immune response against the global minimum anti/anti conformation. Among the possible reasons for the apparent inability of the tetrahydroisoquinoline (THIQ) hapten (MH3 and MH5)-based vaccines to raise sufficient antibody titers, the lower pK_a of the requisite secondary amino group appears to offer one plausible explanation. Furthermore, it seems reasonable to conclude that positioning of the aromatic ring is also a critical determinant of efficacy. In the case of MH1, an anti-anti METH mimetic similar to MH2, the steric repulsion between the aromatic group and the carbonyl group of the MH1 2-piperazinone template resulted in a misalignment of the aromatic ring as compared to the global minimum structure of METH, and in contrast to MH2, which showed a near-perfect fit (Figure 5). Thus, the better fit of the MH2 hapten structure with the global minimum conformation of methamphetamine seems to correlate with the higher titers produced with this hapten. This rationale is further supported by the fact that (1) both of the THIQ haptens which showed poor efficacy also see a misalignment of their aromatic moiety with that of the target structure, and (2) both unconstrained haptens, whose minima structures showed a better fit with that of METH, showed a measurable immune response (Figures 6 and 7).

We note that in contrast to what was expected, bleeds following a third injection showed reduced antibody concentrations. Additional booster injections are usually expected to increase the magnitude of the response as well as focus the antibody population toward the preferred target. In our case, antibody affinity was greatly increased for MH2(R) and MH6 yet remained the same for MH7 across both bleeds. We interpret the decrease in antibody concentration in one of two ways. It is possible that the immune response prior to the last injection was still in the top part of the bell shape curve, and thus upon antigen presentation, part of the current stock of circulating antibodies went to "neutralize the infection", thus reducing the overall antibody concentration. Alternatively, it is possible that overall antibody count was lowered in favor of increasing antibody affinity. We suspect an optimized vaccination schedule wherein animals are allowed a longer "rest" period between injections would be able to rule in favor of one hypothesis.

Amphetamine (amph) is a closely related drug of abuse as well as a METH metabolite; thus, the binding affinity of the antisera for this drug is of interest and was also assayed. Ideally, a clinically viable METH vaccine would produce a response able to provide good recognition for both related structures, thus maximizing its protective effects. Obtaining anti-METH antibodies that cross-react with amphetamine has historically been a challenge with the traditional hapten design, i.e., linker attachment at the aromatic moiety.[28] Gratifyingly, the antisera of MH2(R) (anti-anti constrained METH mimetic) and MH6 (unconstrained hapten) vaccinated animals had moderate affinity for amphetamine which improved upon boosting. MH7, consistent with what has been typically observed with this hapten design,[28] had overall poor affinity (Table 1). The differences

dx.doi.org/10.1021/ja108807j |J. Am. Chem. Soc. 2011, 133, 6587–6595

Table 2. Average Antibody Affinity against Both Isomers of Methamphetamine As Determined by Equilibrium Dialysis

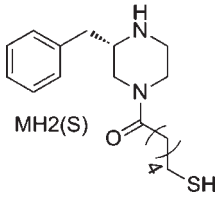

immunized antigen		(+)-METH K_D (μM)	(−)-METH K_D (μM)
MH2 (S)	second bleed	1.720	0.276
MH6	first bleed	0.266	3.050
	second bleed	0.130	2.010

for amphetamine cross-reactivity between MH6 and MH7, both unconstrained cores, is not obvious based on our modeling and is likely the result of an unintended linker effect.

In order to test the importance of retaining the stereochemical requirements of the more potent enantiomer of methamphetamine during hapten design, we synthesized the opposite (S)-enantiomer for the best constrained hapten MH2 (a piperazine core, anti-anti METH mimetic). The response elicited from immunization with MH2(S) was assayed for relative affinity to both isomers of METH. The first bleed contained Abs with little (+)-METH affinity, thus making it difficult to quantify. Gratifyingly, the second bleed antisera of MH2(S) immunized mice had six times better affinity for the (−)-METH isomer as predicted by molecular modeling (Table 2). Furthermore, to prove if stereochemical requirements were also critical for unconstrained METH mimetics, the affinity of MH6 (modeled after (+)-METH) antisera for (−)-METH was measured. MH6 was chosen over MH7 because of its higher antibody concentrations as well as lower binding constants for both METH and AMPH. Competitions with (−)-METH show that MH6 preferentially bound (+)-METH by at least 10-fold (Table 2).

CONCLUSIONS

In summary, the current paper details the rational design of six METH haptens, five with unique structural characteristics, and their ability for precise generation of anti-METH immune responses. Three haptenic compounds, MH2(R), MH6, and MH7, show particular promise in generation of a potentially clinically relevant METH vaccine based on both an elevated antibody titer as well as nanomolar range (+)-METH affinity. Introduction of strategic molecular constraint and stereochemical requirements in MH2(R) allowed for generation of a polyclonal response well within the range of previous monoclonal antibodies tested. Additionally, MH2(R) generated antibodies with moderate affinity for amphetamine, a related drug and methamphetamine metabolite. However, magnitude of the response remained highest in the two unconstrained structures MH6 and MH7. MH6 is of particular interest, as not only did it present a surprisingly high antibody concentration but it also showed good specificity toward METH and discrete affinity toward amphetamine. Further studies including improvements onto the adjuvant activity of the formulations as well as behavioral studies with our prime hapten leads will provide a practical approach toward development of a clinically useful vaccine against methamphetamine abuse.

MATERIALS AND METHODS

Synthetic Generation of Methamphetamine Haptens. Synthetic details for the three haptens of interest are detailed below. Full synthetic detail and characterization of all haptens is given in the Supporting Information.

Synthesis of MH2(R). (*R*)-1-Boc-2-Benzylpiperazine was purchased from Synthonix and used without further purification. A 0.153 mmol amount of 6-(tritylthio)hexanoic acid was mixed with 0.2 mmol of EDC and 0.046 mmol of DMAP in 0.7 mL of DCM. A 0.184 mmol amount of (*R*)-1-Boc-2-benzylpiperazine and 0.3 mmol of 4-methylmorpholine were added, and the reaction mixture was stirred under argon at room temperature for 3 h. The mixture was diluted with ethyl acetate, and the organic layer was washed 3× with saturated sodium bicarbonate, 3× with 10% citric acid, and 1× with water. The organic layer was then dried over sodium sulfate and rotoevaporated. The residue was then passed through a short plug of silica using 80% ethyl acetate/hexane as eluent. The crude product was used without further purification. Global deprotection was achieved by addition of trifluoroacetic acid in a 1:1 dilution with DCM. Drops of triisopropylsilane were added to scavenge the trityl groups. After 2 h, the mixture was rotoevaporated and purified by preparative HPLC. Method = 0−5 min 30%B, to 33%B over 2 min, to 40% B over 27 min, to 95%B over 5 min, hold for 10 min, requilibrate. Product retention time = 13 min. Experimental yield over two steps = 56%. Observed amide rotamers with NMR: ^{1}H NMR (600 MHz, MeOD) δ 7.44−7.24 (m, 13H), 4.58 (s, 1H), 4.44 (s, 1H), 4.08 (d, J = 14.4 Hz, 1H), 3.95 (d, J = 14.5 Hz, 1H), 3.54 (dd, J = 15.6, 12.2 Hz, 1H), 3.50−3.34 (m, 5H), 3.16 (ddd, J = 29.6, 24.5, 15.1 Hz, 2H), 3.05−2.85 (m, 9H), 2.51−2.36 (m, 8H), 2.23 (d, J = 4.2 Hz, 2H), 1.64−1.54 (m, 6H), 1.53−1.46 (m, 3H), 1.43 (d, J = 7.1 Hz, 4H), 1.31 (d, J = 6.9 Hz, 2H). ^{13}C NMR (600 MHz, MeOD) δ = 174.15, 135.89, 130.46, 130.30, 129.03, 128.84, 57.72, 57.41, 49.67, 48.14, 44.70, 43.75, 43.37, 39.37, 37.65, 37.37, 34.93, 34.78, 33.61, 28.99, 25.67, 25.62, 24.87. LRMS $(M + H)^+$: calcd for $C_{17}H_{26}N_2OS$ = 307.18, found 307.1.

Synthesis of MH6. A 0.126 mmol amount of D-amphetamine sulfate was dissolved in 0.9 mL of ethanol. A 0.164 mmol amount of 6-(tritylthio)hexyl methanesulfonate and 0.38 mmol of potassium carbonate were added, and the solution was heated to reflux overnight. After 14 h, ethanol was removed under vacuum and the residue dissolved in ethyl acetate. The organic layer was washed 2× with water, dried over sodium sulfate, and rotoevaporated. The residue was then dissolved in 5 mL of 10% TFA/DCM, and drops of TIS were added as a trityl scavenger. The solution was stirred for 1 h, rotoevaporated, and purified by prep HPLC. Method = 0−5 min 35%B, to 40%B over 2 min, to 44% B over 27 min, to 95%B over 5 min, hold for 10 min, requilibrate. Product retention time = 17 min. Experimental yield over two steps = 50%. ^{1}H NMR (600 MHz, MeOD) δ 7.31 (m, J = 7.5 Hz, 2H), 7.23 (m, 3H), 3.48−3.41 (m, 1H), 3.16 (dd, J = 13.2, 4.4 Hz, 1H), 3.07−2.97 (m, 2H), 2.66 (dd, J = 9.3, 3.9 Hz, 1H), 2.48 (t, J = 7.6 Hz, 1H), 1.73−1.55 (m, 4H), 1.47−1.35 (m, 4H), 1.17 (d, J = 6.6 Hz, 3H). ^{13}C NMR (600 MHz, MeOD) δ = 137.32, 130.41, 130.03, 128.44, 56.95, 49.61, 46.31, 40.35, 39.22, 34.85, 29.88, 28.92, 28.82, 27.47, 27.26, 27.11, 24.79, 16.07. LRMS $(M + H)^+$: calcd for $C_{15}H_{25}NS$ = 252.17, found 252.2.

Synthesis of MH7 (four steps). *Synthesis of (S)-2,2,2-Trifluoro-N-methyl-N-(1-(4-nitrophenyl)propan-2-yl)acetamide.* A 0.269 mmol amount of D-methamphetamine hydrochloride was dissolved in 1.8 mL DCM. A 0.538 mmol amount of triethylamine was added, and the mixture was cooled to 0 °C. A 0.323 mmol amount of trifluoroacetic anhydride was added dropwise, and the mixture was stirred at room temperature for 2.5 h. The solvent was removed under vacuum and the residue dissolved in ethyl ether which resulted in the formation of a precipitate. The solution was passed through a short plug of silica topped with basic alumina. The filtrates

dx.doi.org/10.1021/ja108807j |*J. Am. Chem. Soc.* 2011, 133, 6587–6595

were combined and rotoevaporated to yield a single spot by TLC which was carried forward without further purification. The residue was dissolved in 0.51 mL of DCM and added dropwise to a chilled solution consisting of 3.26 mmol of potassium nitrate and 3.09 mmol of concentrated sulfuric acid previously dissolved in 1.63 mL of DCM. The slurry was stirred overnight at room temperature. An aqueous solution of sodium sulfate was used to quench the reaction. The two layers were separated, and the organic layer was washed twice more with aqueous sodium sulfate. Organics were combined, dried with anhydrous sodium sulfate, and rotoevaporated. The product was purified using silica chromatography with 10% ethyl acetate/hexane as the eluent. The major product of reaction was para-substituted as evidenced by NMR. Experimental yield = 54% (para). TLC conditions 15% EtOAc/hex R_f = 0.16. Observed rotamers 1:0.5 by NMR; shifts and integration given for main rotamer: ^{1}H NMR (600 MHz, $CDCl_3$) δ 8.17 (d, J = 8.7 Hz, 2H), 7.36 (d, J = 8.6 Hz, 2H), 4.87 (dq, J = 13.8, 6.9 Hz, 1H), 3.00−2.90 (m, 5H), 1.29−1.25 (m, 3H). ^{13}C NMR (600 MHz, $CDCl_3$) δ = 176.84, 147.35, 147.20, 145.28, 144.79, 130.04, 129.90, 124.24, 124.05, 54.10, 52.40, 40.92, 39.50, 29.92, 29.37, 28.23, 18.49, 17.08. LRMS $(M + H)^+$: calcd for $C_{12}H_{13}F_3N_2O_3$= 291.09, found 291.4.

Synthesis of (S)-N-(1-(4-Aminophenyl)propan-2-yl)-2,2,2-trifluoro-N-methylacetamide. A 0.174 mmol amount of (*S*)-2,2,2-trifluoro-*N*-methyl-*N*-(1-(4-nitrophenyl)propan-2-yl)acetamide was dissolved in MeOH, and 12 mg of 10% activated palladium on carbon was added under a hydrogen balloon. The reaction was stirred for 2 h before being filtered on a Celite plug. The plug was washed with methanol, filtrates were combined, and solvent was removed under vacuum. The residue was purified using silica chromatography using 20% ethyl acetate/hexane as eluent. Experimental yield = 97%. TLC conditions 30% EtOAc/hex R_f = 0.3. Observed rotamers by NMR 1:0.7; shifts and integration given for main rotamer: ^{1}H NMR (500 MHz, $CDCl_3$) δ 6.95 (d, J = 8.2 Hz, 2H), 6.66−6.59 (m, 2H), 4.82−4.70 (m, 1H), 3.60 (broad s, 2H), 2.92 (s, 3H), 2.83−2.62 (m, 2H), 1.29−1.17 (m, 3H). ^{13}C NMR (500 MHz, $CDCl_3$) δ = 183.74, 145.33, 143.76, 130.13, 130.00, 127.62, 115.69, 115.63, 54.92, 53.03, 40.58, 38.97, 28.31, 18.17, 16.90. LRMS $(M + H)^+$: calcd for $C_{12}H_{15}F_3N_2O$ = 261.11, found 261.1.

Synthesis of (S)-N-(4-(2-(2,2,2-trifluoro-N-methylacetamido)propyl)-phenyl)-6-(tritylthio)hexanamide. A 0.172 mmol amount of (*S*)-*N*-(1-(4-aminophenyl)propan-2-yl)-2,2,2-trifluoro-*N*-methylacetamide was dissolved in 0.368 mL of DCM. A 0.157 mmol amount of 6-(tritylthio)hexanoic acid, 0.204 mmol of EDC, and 0.047 mmol of DMAP were added, and the mixture was stirred. A 0.314 mmol amount of 4-methylmorpholine was added, and the reaction was stirred for 4 h. A 3 mL volume of ethyl acetate was added and washed 2× with saturated sodium bicarbonate, 4× with 10% citric acid, and 1× with water. The organic layer was dried over sodium sulfate and rotoevaporated to a yellow oil which corresponded to single spot on TLC. Experimental yield = 93%. TLC conditions 20% EtOAc/hex R_f = 0.13. Observed amide rotamers at a ratio of 1:0.63. ^{1}H NMR (600 MHz, $CDCl_3$) δ 7.41 (dd, J = 12.7, 8.7 Hz, 13H), 7.27 (dd, J = 10.5, 4.3 Hz, 12H), 7.20 (t, J = 7.6 Hz, 4H), 7.16−7.04 (m, 5H), 4.85−4.73 (m, 1H), 2.91 (s, J = 25.0 Hz, 5H), 2.87−2.70 (m, 3H), 2.25 (dd, J = 12.1, 7.2 Hz, 3H), 2.16 (t, J = 6.9 Hz, 3H), 1.64−1.53 (m, 4H), 1.45−1.38 (m, 3H), 1.37−1.27 (m, 4H), 1.21 (t, J = 7.0 Hz, 7H). ^{13}C NMR (600 MHz, $CDCl_3$) δ = 171.16, 145.14, 136.95, 136.73, 129.76, 129.67, 129.53, 128.02, 126.74, 120.19, 120.03, 66.65, 54.55, 52.67, 40.61, 39.01, 37.64, 31.92, 28.66, 28.63, 28.49, 28.18, 25.22, 18.08, 16.81. LRMS $(M + Na)^+$: calcd for $C_{37}H_{39}F_3N_2O_2S$ = 655.25, found 655.3.

Synthesis of MH7. A 0.145 mmol amount of (*S*)-*N*-(4-(2-(2,2,2-trifluoro-*N*-methylacetamido)propyl)phenyl)-6-(tritylthio)hexanamide was dissolved in 1 mL of methanol and drops of water. A 0.436 mmol amount of potassium carbonate was added and the mixture stirred at room temperature for 50 h. The methanol was removed under vacuum, and the residue was dropped in water. The aqueous layer was basified and extracted 3× with DCM. The organic layers were combined, dried over sodium sulfate, and rotoevaporated. The residue was dissolved in 6 mL of 10% TFA/DCM, and drops of TIS were added to scavenge the trityl groups. The solution was stirred for 1 h, rotoevaporated, and purified by prep HPLC. Method = 0−5 min 25%B, to 30%B over 2 min, to 40% B over 27 min, to 95%B over 5 min, hold for 10 min, requilibrate. Product retention time = 19 min. Experimental yield over two steps = 40%. ^{1}H NMR (500 MHz, MeOD) δ 7.54 (dd, J = 8.6, 2.4 Hz, 2H), 7.21 (d, J = 8.5 Hz, 2H), 3.48−3.40 (m, 1H), 3.34 (s, 1H), 3.07 (dd, J = 13.7, 5.3 Hz, 1H), 2.71 (s, 3H), 2.51 (t, J = 7.6 Hz, 2H), 2.37 (t, J = 7.5 Hz, 2H), 1.74−1.61 (m, 4H), 1.52−1.45 (m, 2H), 1.23 (d, J = 6.6 Hz, 3H). ^{13}C NMR (500 MHz, MeOD) δ = 130.81, 121.84, 57.81, 39.71, 37.81, 34.88, 30.95, 28.95, 26.35, 24.83, 15.80. LRMS $(M + H)^+$: calcd for $C_{16}H_{26}N_2OS$ = 295.18, found 295.2.

Hapten−Protein Immunoconjugates. Immunoconjugates were prepared by reaction of the thiol presenting haptens with maleimide-activated protein, either KLH or BSA. Briefly, protein activation was accomplished by reacting 1 mg of protein with 1 mg of S-GMBS (*N*-[γ-maleimidobutyryloxy]sulfosuccinimide ester, Pierce) at a concentration of 5.4 mg protein/mL of EDC conjugation buffer. The solution was shaken at room temperature for 3 h and dialyzed thoroughly in order to remove unreacted material. The concentration of the activated solution was determined via the BCA assay. Preweighed haptens were then dissolved directly into the protein solution at a ratio of 0.5 mg of hapten:1 mg of protein. The mixture was shaken for 30 min at room temperature followed by overnight shaking at 4 °C. The solution was once again dialyzed and characterized. Coupling efficiencies were monitored using MALDI-TOF MS for all BSA conjugates. Because of the size of KLH, conjugates to this protein could not be directly analyzed. For BSA, all haptens showed similar coupling efficiencies of about 24−29 copies per BSA protein molecule.

Vaccination Protocols for Mice Studies. Groups of n = 4 129GI^x mice (6−8 weeks, 23−28 g) were immunized i.p. on days 0, 14, and 35 with a suspension of each hapten−KLH conjugate (100 μg) in formulation with Sigma Adjuvant System (SAS, Sigma) according to the manufacturer's instructions. SAS is a stable oil-in-water emulsion that may be used as an alternative to the classical Freund′s water-in-oil emulsions. This adjuvant is derived from bacterial and mycobacterial cell wall components such as detoxified monophosphoryl lipid A derived from *Salmonella minnesota* and synthetic trehalose dicorynomycolate that provide a potent stimulus to the immune system. Following vaccine administration, serum (0.1 mL) was collected on days 21 and 42 via tail-bleed. All biological samples were stored at −80 °C until use to preserve integrity.

Immunoassays: ELISA. Production of methamphetamine-specific IgG was initially monitored by ELISA using MH6− and MH7−BSA conjugates as the coating antigen. Titers were calculated from the plot of absorbance versus log dilution and were defined as the dilution corresponding to an absorbance reading 50% of the maximal value. MH6−BSA, MH7−BSA, and protein only controls were added individually to COSTAR 3690 microtiter plates and allowed to dry at 37 °C overnight. Following methanol fixation, nonspecific binding was blocked with a solution of 5% nonfat powdered milk in PBS for 0.5 h at 37 °C. Next, mouse sera was serially diluted in a 1% BSA solution across the plate and allowed to incubate for 1−2 h at 37 °C in a moist chamber. Plates were then washed with DI H_2O and treated with goat antimouse-HRP antibody for 0.5 h at 37 °C. Following another wash cycle, plates were developed with the TMB two-step kit (Pierce; Rockford, IL).

Equilibrium Dialysis. Refined values for antibody affinity, specificity, and concentration were determined using a solution-based radioimmunoassay (RIA). A modified version of Muller's method[29] was followed, as it allows for determination of both affinity constant and concentration of specific antibody in serum. The RIA was carried out in a 96-well equilibrium dialyzer MWCO 5000 Da (Harvard Apparatus, Holliston, MA) to allow easy separation of bound and free (+)-[2′,6′-

3H(n)] methamphetamine tracer; specific activity = 39 Ci/mmol (obtained from the National Institute on Drug Abuse (Bethesda, MD) and synthesized at Research Triangle Institute (Research Triangle Park, NC). Briefly, mouse sera for each bleed for each hapten were pooled together and diluted in RIA buffer (sterile filtered 2% BSA in 1× PBS pH = 7.4) to a concentration that would bind 11−30% of ∼24 000 decays/min of 3*H*-methamphetamine tracer. A 100 μL aliquot of sera was combined with 50 μL of radiolabeled tracer (∼24 000 decays/min) and 150 μL of unlabeled competitor [(+)-methamphetamine or (+)-amphetamine] at varying concentrations in PBS pH = 7.4 was added to the solvent chamber, and the samples were allowed to reach equilibrium on a plate rotator (Harvard Apparatus, Holliston, MA) at room temperature for at least 22 h. A 100 μL aliquot from each sample/solvent chamber was slowly aspirated and suspended in 5 mL of scintillation fluid (Ecolite, ICN, Irvine, CA), and the radioactivity of each sample was determined by liquid scintillation spectrometry.

■ ASSOCIATED CONTENT

Supporting Information. Complete synthetic routes and characterization of chemical compounds as well as binding competition curves. This material is available free of charge via the Internet at http://pubs.acs.org.

■ AUTHOR INFORMATION

Corresponding Author
kdjanda@scripps.edu

■ ACKNOWLEDGMENT

The authors appreciate the financial support provided by NIDA (DA024705) and The Skaggs Institute for Chemical Biology. (+)-[2′,6′-3H(n)] methamphetamine for soluble radioimmunoassays was obtained from the National Institute on Drug Abuse (Bethesda, MD) and synthesized at Research Triangle Institute (Research Triangle Park, NC).

■ REFERENCES

(1) Gonzales, R.; Mooney, L.; Rawson, R. A. *Annu. Rev. Public Health* **2010**, *31*, 385–98.

(2) Nicosia, N.; Pacula, R. L.; Kilmer, B.; Lundberg, R.; Chiesa, J. *The Economic Cost of Methamphetamine Use in the United States, 2005*; RAND Corporation: Santa Monica, CA, 2009. http://www.rand.org/pubs/monographs/MG829.

(3) Treweek, J. B.; Dickerson, T. J.; Janda, K. D. *Acc. Chem. Res.* **2009**, *42* (5), 659–669.

(4) Meijler, M. M.; Matsushita, M.; Wirsching, P.; Janda, K. D. *Curr. Drug Discovery Technol.* **2004**, *1* (1), 77–89.

(5) Karila, L.; Weinstein, A.; Aubin, H.-J.; Benyamina, A.; Reynaud, M.; Batki, S. L. *Br. J. Clin. Pharmacol.* **2010**, *69* (6), 578–592.

(6) (a) Kantak, K. M. *Drugs* **2003**, 341–352. (b) Meijler, M.; Matsushita, M.; Wirsching, P.; Janda, K. D. *Curr. Drug Discovery Technol.* **2004**, *1*, 77–89. (c) Kosten, T.; Owens, S. M. *Pharmacol. Ther.* **2005**, *108* (1), 76–85.

(7) (a) Cornuz, J.; Zwahlen, S.; Jungi, W. F.; Osterwalder, J.; Klingler, K.; van Melle, G.; Bangala, Y.; Guessous, I.; Muller, P.; Willers, J.; Maurer, P.; Bachmann, M. F.; Cerny, T. *PLoS ONE* **2008**, *3* (6), e2547. (b) Hatsukami, D. K.; Rennard, S.; Jorenby, D.; Fiore, M.; Koopmeiners, J.; de Vos, A.; Horwith, G.; Pentel, P. R. *Clin. Pharmacol. Ther.* **2005**, *78* (5), 456–467.

(8) (a) Haney, M.; Gunderson, E. W.; Jiang, H.; Collins, E. D.; Foltin, R. W. *Biol. Psychiatry* **2010**, *67* (1), 59–65. (b) Martell, B. A.; Orson, F. M.; Poling, J.; Mitchell, E.; Rossen, R. D.; Gardner, T.; Kosten, T. R. *Arch. Gen. Psychiatry* **2009**, *66* (10), 1116–1123.

(9) Byrnes-Blake, K. A.; Carroll, F. I.; Abraham, P.; Owens, S. M. *Int. Immunopharmacol.* **2001**, *1*, 329–338.

(10) Ino, A.; Dickerson, T. J.; Janda, K. D. *Bioorg. Med. Chem. Lett.* **2007**, *17* (15), 4115–4121.

(11) (a) Owens, S. M.; Zorbas, M.; Lattin, D. L.; Gunnell, M.; Polk, M. *J. Pharmacol. Exp. Ther.* **1988**, *246* (2), 472–478. (b) Matsushita, M.; Hoffman, T. Z.; Ashley, J. A.; Zhou, B.; Wirsching, P.; Janda, K. D. *Bioorg. Med. Chem. Lett.* **2001**, *11* (2), 87–90.

(12) Peterson, E. C.; Gunnell, M.; Che, Y.; Goforth, R. L.; Carroll, F. I.; Henry, R.; Liu, H.; Owens, S. M. *J. Pharmacol. Exp. Ther.* **2007**, *322*, 30–39.

(13) Duryee, M. J.; Bevins, R. A.; Reichel, C. M.; Murray, J. E.; Dong, Y.; Thiele, G. M.; Sanderson, S. D. *Vaccine* **2009**, *27*, 2981–2988.

(14) Gentry, W. B.; Ruedi-Bettschen, D.; Owens, S. M. *Hum. Vaccines* **2009**, *5* (4), 206–213.

(15) Kaminski, G. A.; Friesner, R. A.; Tirado-Rives, J.; Jorgensen, W. L. *J. Phys. Chem. B* **2001**, *105*, 6474–6487.

(16) Still, W. C.; Tempczyk, A.; Hawlely, R. C.; Hendrickson, T. A. *J. Am. Chem. Soc.* **1990**, *112*, 6127–6129.

(17) Kolossváry, I.; Guida, W. C. *J. Comput. Chem.* **1999**, *20*, 1671.

(18) David, R. L. *Handbook of Chemistry and Physics*, 90th ed.; CRC Press: New York, NY, 2009−2010; p 2804.

(19) Huizing, G.; Beckett, A. *Pharm. World Sci.* **1980**, *2* (1), 253–261.

(20) Beaumont, D.; Waigh, R. D.; Sunbhanich, M.; Nott, M. W. *J. Med. Chem.* **1983**, *26* (4), 507–515.

(21) Shelley, J.; Cholleti, A.; Frye, L.; Greenwood, J.; Timlin, M.; Uchimaya, M. *J. Comput.-Aided Mol. Des.* **2007**, *21* (12), 681–691.

(22) Meijler, M. M.; Matsushita, H.; Atobell, L. J.; Wirshing, P.; Janda, K. D. *J. Am. Chem. Soc.* **2003**, *125*, 7164–7165.

(23) Dewey, S. L.; Kroll, C.; Ferrieri, R.; Schiffer, W.; Alexoff, D.; Shea, D.; Youwen, C. X.; Muench, L.; Volkow, L.; Fowler, J. . *J. Nucl. Med. Meeting Abstr.* **2006**, *47*, 135P-b.

(24) (a) Mendelson, J.; Uemura, N.; Harris, D.; Nath, R.; Fernandez, E.; Jacob, P. I.; Everhart, E. T.; Jones, R. T. *Clin. Pharmacol. Ther.* **2006**, *80* (4), 403–420. (b) Wang, Z.; Woolverton, W. L. *Psychopharmacology* **2007**, *189* (4), 483–488.

(25) Janda, K. D.; Benkovic, S. J.; Lerner, R. A. *Science* **1989**, *244*, 437–440.

(26) Laurenzana, E. M.; Hendrickson, H. P.; Carpenter, D.; Peterson, E. C.; Gentry, W. B.; West, M.; Che, Y.; Carroll, F. I.; Owens, S. M. *Vaccine* **2009**, *27* (50), 7011–7020.

(27) Keyler, D. E.; Roiko, S. A.; Earley, C. A.; Murtaugh, M. P.; Pentel, P. R. *Int. Immunopharmacol.* **2008**, *8*, 1589–1594.

(28) Carroll, F. I.; Abraham, P.; Gong, P. K.; Pidaparthi, R. R.; Blough, B. E.; Che, Y.; Hampton, A.; Gunnell, M.; Lay, J. O., Jr.; Peterson, E. C.; Owens, S. M. *J. Med. Chem.* **2009**, *52* (22), 7301–9.

(29) Muller, R. *Methods Enzymol.* **1983**, *92*, 589–601.